Anal. Chem. **2006,** *78,* 2816−2822

Fabrication of Optically Transparent Carbon Electrodes by the Pyrolysis of Photoresist Films: Approach to Single-Molecule Spectroelectrochemistry

Sebastian Donner, Hung-Wing Li, Edward S. Yeung, and Marc D. Porter*

Ames Laboratory—U.S.D.O.E., Departments of Chemistry and of Chemical and Biological Engineering, and Institute for Combinatorial Discovery, Iowa State University, Ames, Iowa 50011

This paper describes the preparation, physical and chemical characterization, and performance of carbon-based optically transparent electrodes (C-OTEs) fabricated by the pyrolysis of thin films of photoresist. The electrodes are prepared by spin coating dilute solutions of the positive photoresist AZ 4330 onto quartz substrates. Pyrolysis of these samples at 1000 °C in a reducing atmosphere yields optically transparent carbon films that have thicknesses ranging between 10 and 80 nm. Sheet resistance measurements, X-ray photoelectron spectroscopy, Raman spectroscopy, and atomic force microscopy were used to determine the physical and chemical properties of the films, and cyclic voltammetry and chronoabsorptometry were employed to delineate the electrochemical and conventional spectroelectrochemical performance of the C-OTEs. These findings showed that the transparency of this material improves as film thickness decreases, but at the expense of an increase in film resistance. At a wavelength of 500 nm, for example, 13- and 79-nm-thick films have transparencies of 47 and 10% and sheet resistances of 1100 and 210 Ω/□, respectively. Importantly, adjusting the dilution factor allows the facile and reproducible variation of thickness and transparency. Preliminary results using these C-OTEs for single-molecule spectroelectrochemistry, which represents a new development in the merger of optical and electrochemical techniques, by probing the potential dependence of the adsorption of individual YOYO-I-labeled λ-DNA are also presented.

Optically transparent electrodes (OTEs) have proven invaluable to a wide range of investigations of electrochemical processes.[1−4] The design and synthesis of OTEs have traditionally relied on the deposition of conductive thin films such as indium and tin oxide, gold, platinum, and to lesser extents, mercury, carbon, and doped diamond on a suitably transparent substrate.[1−8] Metallic microscreens, referred to as minigrid electrodes, have also been employed.[9] The vast majority of work on OTEs has focused on materials that can be applied in the visible region of the electromagnetic spectrum. In a few cases, however, access to infrared wavelengths has been achieved by either the deposition of germanium on an infrared transparent material[5] or the incisive doping of diamond film electrodes.[8]

The design of a film-based OTE represents a tradeoff between optical transparency and electrical resistivity, both of which are controlled by film thickness.[6] Film-based OTEs must be sufficiently thin, typically tens of nanometers, to be optically transparent. However, most electrode materials have large internal resistances at such thicknesses, which can distort the electrochemical response because of a distribution of the applied potential across the electrode surface. Thin film electrodes may also be mechanically fragile, posing handling problems.

This paper describes a novel approach to the facile fabrication of carbon-based OTEs (C-OTEs). Carbon is attractive as an electrode material because of its wide potential window, low background current, and low cost. Part of our interest in this area stems from the use of carbon as a detector in sensor applications.[10] The work herein, however, was largely motivated by our continued development of electrochemically modulated liquid chromatography (EMLC).[11] EMLC is a form of high performance liquid chromatography in which the LC column is modified to also function as an electrochemical cell. The manipulation of the potential applied (E_{app}) to a conductive stationary-phase-like glassy carbon or porous graphitic carbon alters the surface charge density of the packing, which, in turn, fine-tunes analyte retention.

* Corresponding author. E-mail: mporter@porter1.ameslab.gov. Phone: 515-294-6433.

(1) Kuwana, T.; Winograd, N. In *Electroanalytical Chemistry*; Bard, A. J., Ed.; Marcel Dekker: New York, 1974; Vol. 7, pp 1−78.
(2) Heineman, W. R.; Hawkridge, F. M.; Blount, H. N. *Electroanal. Chem.* **1984**, *13*, 1−113.
(3) Stotter, J.; Haymond, S.; Zak, J. K.; Show, Y.; Cvackova, Z.; Swain, G. M. *Electrochem. Soc. Interface* **2003**, *12*, 33−38.
(4) Zudans, I.; Paddock, J. R.; Kuramitz, H.; Maghasi, A. T.; Wansapura, C. M.; Conklin, S. D.; Kaval, N.; Shtoyko, T.; Monk, D. J.; Bryan, S. A.; Hubler, T. L.; Richardson, J. N.; Seliskar, C. J.; Heineman, W. R. *J. Electroanal. Chem.* **2004**, *565*, 311−320.
(5) Mattson, J. S.; Smith, C. A. *Anal. Chem.* **1975**, *47*, 1122−1125.
(6) Haacke, G. *Annu. Rev. Mater. Sci.* **1977**, *7*, 73−93.
(7) DeAngelis, T. P.; Hurst, R. W.; Yacynych, A. M.; Mark, H. B.; Heineman, W. R.; Mattson, J. S. *Anal. Chem.* **1977**, *49*, 1395−1398.
(8) Haymond, S.; Zak, J. K.; Show, Y.; Butler, J. E.; Babcock, G. T.; Swain, G. M. *Anal. Chim. Acta* **2003**, *500*, 137−144.
(9) Petek, M.; Neal, T. E.; Murray, R. W. *Anal. Chem.* **1971**, *43*, 1069−1074.
(10) Hong, H.; Porter, M. D. *J. Electroanal. Chem.* **2005**, *578*, 113−119.
(11) Harnisch, J. A.; Porter, M. D. *Analyst* **2001**, *126*, 1841−1849.

10.1021/ac052244d CCC: $33.50
Published on Web 03/16/2006

In previous work, we have shown that measurements of retention with respect to changes in E_{app} can be employed to gain thermodynamic insights into the separation mechanism at carbonaceous packings.[12,13] It follows that this type of measurement can also be exploited as a tool to probe fundamental issues central to adsorption at electrified interfaces. However, perspectives gained by such measurements reflect the integrated response of a large ensemble of analytes over a large, potentially diverse population of adsorption sites. Several studies have, in fact, amply demonstrated that the most used type of carbon electrode material, glassy carbon, has a surface that is both chemically and physically heterogeneous.[14,15]

In an effort to probe adsorption at electrified interfaces on a much smaller length scale, this paper details the design, fabrication, and preliminary testing of C-OTEs suitable not only for conventional spectroelectrochemical applications but also for investigations by single-molecule spectroscopy. Earlier reports on the fabrication of C-OTEs have primarily employed the resistive sputtering and vapor deposition of carbon[7,16] or the pyrolysis of organic thin films.[17] The work described herein takes a slightly different tactic by preparing C-OTEs via the pyrolysis of thin films of photoresist. We show that this approach, which extends advances recently detailed by other laboratories for the preparation of much thicker (i.e., nontransparent) carbon film electrodes,[18−21] yields mechanically robust, amorphous carbon coatings that are optically transparent at thicknesses less than ∼80 nm. Herein, we detail the findings from characterizations of the transmittance, electrical resistivity, surface composition, and topographic roughness of this new form of C-OTE, along with preliminary applications in both conventional and single-molecule spectroelectrochemistry. The latter application represents, to our knowledge, the first example of the union of electrochemistry and single-molecule spectroscopy.

EXPERIMENTAL SECTION

C-OTE Fabrication. The procedure for the fabrication of our C-OTEs consists of five steps. It represents a minor modification of the procedure detailed by the Kinoshita[19] and McCreery laboratories[20] for the preparation of much thicker (i.e., nontransparent) carbon electrodes via the pyrolysis of photoresist films. The major difference is that the starting material was diluted with its solvent to decrease its viscosity to allow the casting of a thinner film. In step 1, quartz slides (Technical Glass) are rinsed rigorously with acetone and 2-propanol and dried under a stream of high-purity nitrogen.

In step 2, the positive photoresist AZ P4330−RS (Clarian) is diluted with 1-methoxy-2-propanol acetate to 25−50% (v/v) of the as-received material. Dilution reduces the viscosity of the resist solution to levels needed to cast films sufficiently thin to exhibit optical transparency after pyrolysis.

Step 3 spin coats the diluted photoresist at 6000 rpm for 30 s onto a quartz substrate, and step 4 "soft bakes" the coated substrate at 110 °C for 60 s in a muffle furnace.

In step 5, the sample is pyrolyzed in a furnace (Lindberg Blue M model 54253) that is fitted with a hard-fired alumina tube. This step begins by flushing the system at 1000 sccm with forming gas (95:5% nitrogen/hydrogen (v/v)) for 5 min, temporarily pumping the system down to 200 mTorr, and flowing the forming gas through the system for an additional 10 min. Next, the sample is pyrolyzed by ramping the temperature to 1000 °C at 10 °C/min. The temperature is held at 1000 °C for 1 h while continuously flowing the forming gas at 1000 sccm through the alumina tube. The system is then allowed to radiatively cool to room temperature while maintaining the flow of forming gas. After terminating the flow of forming gas, the alumina tube is backfilled with high-purity nitrogen.

Samples were stored before use in a glass microscope slide carrier for a minimum of 3 days, which reflects earlier observations that the spontaneous surface oxidation of much thicker pyrolyzed films of the photoresist levels off after 3 days of air exposure.[22] The electrodes adhered strongly to the substrate. For example, extended sonication in various solvents had no effect on the surface. Moreover, the surface is mechanically rugged, requiring a sharp stylus to leave striations. However, the material does occasionally delaminate after extensive application of an applied potential at the limits of the working potential window (i.e., values of E_{app} less than −1.0 V or greater than E_{app} +1.0 V, 1.0 M KCl).

Material Characterizations. Sheet resistance measurements were performed with a Keithley 2400 Source Meter that was connected through a breakout box to a probe card mounted on a microscope. This setup provided the capability of performing four-point probe determinations of sheet resistance. The voltage drop was measured at four or more different locations on each sample to determine the average film resisitivity and its lateral variation.

Film thicknesses were assessed with a surface profilometer (Dektak IIA, Sloan), using samples photolithographically patterned to expose the underlying substrate prior to pyrolysis. The procedure first soft-baked the resist for 60 s at 110 °C. The next step used a positive transparency mask with varied sized features (50, 100, and 350 μm) for the localized patterning and exposure of the samples to a UV flood source. The resist was then immersed in a 1:5 (v/v) dilution of AZ 400K developer in water for 45 s, dried under a stream of high-purity nitrogen, and imaged by atomic force microscopy (AFM) after pyrolysis. There was no visible or microscopic evidence that the development step etched the underlying quartz substrate.

The surface roughnesses of the films were assessed using a NanoScope III AFM (Digital Instruments) with silicon TESP probe tips (Nanosensors). All absorbance measurements were carried out with an HP 8453 UV−visible spectrometer and were corrected for contributions from the supporting quartz substrate.

Electrochemical experiments employed a Bipotentiostat model AFCBP1 (Pine), a silver/silver chloride (Ag/AgCl, saturated KCl) reference electrode, and a platinum wire as the counter electrode.

(12) Ponton, L.; Porter, M. D. *Anal. Chem.* **2004**, *76*, 5823−5828.
(13) Keller, D. W.; Porter, M. D. *Anal. Chem.* **2005**, *77*, 7399−7407.
(14) Randin, J. P.; Yeager, E. *Electroanal. Chem. Interfacial Electrochem.* **1975**, *58*, 313−322.
(15) McCreery, R. L. In *Interfacial Electrochemistry*; Wieckowski, A., Ed.; Marcel Dekker: New York, 1999; pp 631−647.
(16) Dawson, J. C.; Adkins, C. J. *J. Phys.: Condens. Matter* **1995**, *7*, 6297−6315.
(17) Anjo, D. M.; Brown, S.; Wang, W. *Anal. Chem.* **1993**, *65*, 317−319.
(18) Lyons, A. M. *J. Non-Cryst. Solids* **1985**, *70*, 99−109.
(19) Kim, J.; Song, X.; Kinoshita, K.; Madou, M.; White, R. *J. Electrochem. Soc.* **1998**, *145*, 2314−2319.
(20) Ranganathan, S.; McCreery, R. L.; Majji, S. M. a.; Madou, M. *J. Electrochem. Soc.* **2000**, *147*, 277−282.
(21) Kostecki, R.; Schnyder, B.; Alliata, D.; Song, X.; Kinoshita, K.; Koetz, R. *Thin Solid Films* **2001**, *396*, 36−43.
(22) Ranganathan, S.; McCreery, R. L. *Anal. Chem.* **2001**, *73*, 893.

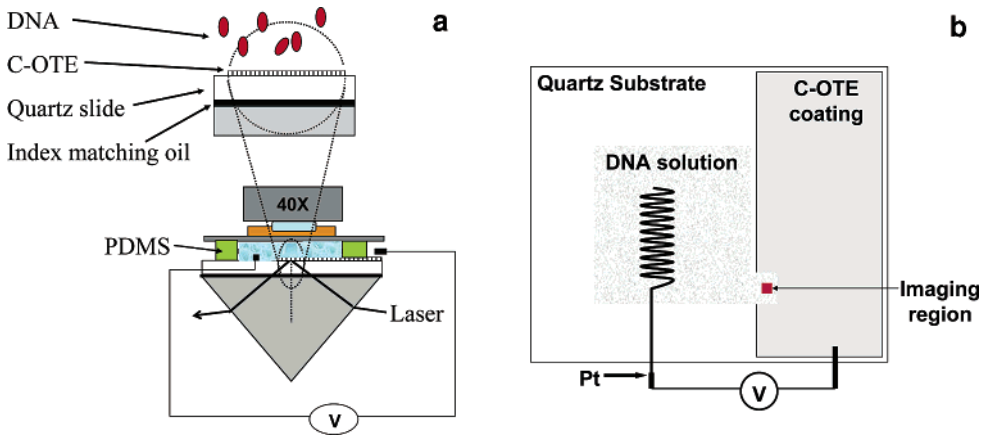

Figure 1. (a) Side view of single-molecule spectroscopy setup (partial) with expanded view of the detection region. (b) Top view of electrochemical cell. PDMS confining the DNA solution and the glass cover slide are not shown.

Ferrocyanide (Aldrich) and hydroxymethylferrocene (Aldrich) were used as test redox couples, which both have approximate formal reduction potentials of +0.225 V (vs Ag/AgCl, saturated KCl) in 1.0 M potassium chloride (Aldrich). These experiments were performed without *iR* compensation.

Spectroelectrochemistry. Conventional spectroelectrochemical studies used a cell based on the classic design of Kuwana and Winograd[1] in which the probe beam is oriented normal to the electrode surface. A 0.6-cm-diameter O-ring, which sealed the electrode to the cell, defined the geometric area of the electrode (0.28 cm^2) exposed to solution. Electrical contact to the C-OTEs was made with adhesive copper tape, cut to have a circular opening slightly larger than the O-ring. The analyte was 10.0 mM ferrocyanide in 1.0 M potassium chloride. In these experiments, performed in a chronoabsoptometry mode, the absorption at 420 nm was used to follow the formation of ferricyanide when the applied potential was changed from 0.00 to +0.60 V.

The instrumental setup for the evanescent-wave excitation geometry used for single-molecule spectroelectrochemistry is partially shown in Figure 1a.[23] A detailed view of the spectroelectrochemical cell is given in Figure 1b. The setup entails the addition of 20 μL of 50 pM YOYO-I-labeled λ-DNA in 10 mM Gly−Gly buffer (pH 8.2) into a reservoir defined by a molded housing fashioned from a 150-μm-thick block of poly(dimethylsiloxane) (PDMS), a No. 1 (170-μm-thick) Corning glass coverslip, and a 35-nm-thick C-OTE. A dc power supply (Array Electronic) and a two-electrode system were used. A platinum wire served as the counter electrode, while the positive lead of the power supply was connected to the C-OTE with adhesive copper tape. The assembly was placed on the prism with index-matching oil to achieve airless contact. A laser beam was focused and directed through the prism at an angle of incidence of ~66° with respect to the quartz slide/sample interface. The laser beam was totally internally reflected at the C-OTE/solution interface, creating an evanescent field with a penetration depth of 110−120 nm. Fluorescent molecules within this field can therefore be excited and imaged.

An argon ion laser (Innova-90, Coherent) was operated at 488 nm as the excitation source. Extraneous light and plasma lines from the laser were removed by an equilateral prism and a pinhole placed prior to the entrance to the observation region. The total laser power, prior the prism, was ~10 mW. The microscope objective was a Zeiss 40× Plan-Neofluar (oil 1.3 NA). The objective was coupled to the coverslip with immersion oil (type FF, n = 1.48, Cargille). Images of the irradiated region were recorded with an intensified CCD camera (Cascade, Roper Scientific). The camera was held at −35 °C.

A 488-nm holographic notch filter (Kaiser Optical) with an optical density of >6 was placed between the objective and CCD camera. The digitization rate of the CCD camera was 1 MHz (16 bits). The digital−analog converter setting was 3689. The frame-transfer function of the CCD camera was operated in the external synchronization mode, with the exposure timing for the camera and laser shutter synchronized by a shutter driver/timer (Uniblitz ST132, Vincent Associates). The CCD exposure frequency was 1 Hz. The exposure time for each frame was 10 ms. A sequence of frames were acquired in each experiment via V^{2+} software (Roper Scientific).

λ-DNA (48 502 bp, fully extended length of ~16 μm, Life Technologies) samples were prepared in 10 mM Gly−Gly buffer at pH 8.2. The DNA samples were labeled using a ratio of one YOYO-I (Molecular Probes) dye molecule per five base pairs. The Gly−Gly buffer solutions were previously photobleached under a mercury lamp for ~12 h and passed through a 0.2-μm filter. Quantification was achieved using counting software.

RESULTS AND DISCUSSION

Material Characterization. The results from several characterizations of the material properties (i.e., thickness, roughness, transmittance, and sheet resistance) of our C-OTEs are presented in Table 1 and Figures 2−4. The results and discussion from X-ray photoelectron and Raman spectroscopy studies are provided as Supporting Information.

Film Thicknesses. Table 1 summarizes the dependence of the pyrolyzed film thickness as a function of photoresist concentration and number of coatings. As expected, the pyrolyzed film thickness increases with photoresist concentration and the number of coating depositions. A coating cast once from a 50% dilution, for example, yields a thickness of 70 ± 0.4 nm, whereas that from a 25% dilution is 13 ± 0.7 nm. The number of depositions prior to pyrolysis can also be used to manipulate the film thickness. Multiple depositions of the photoresist lead to small, but readily

(23) Kang, S. H.; Shortreed, M. R.; Yeung, E. S. *Anal. Chem.* **2001**, *73*, 1091−1099.

Table 1. Thickness of C-OTEs as a Function of AZ 4330 Concentration and Number of Depositions

AZ 4330 concn (% V)	no. of coatings[a]	PPF thickness (nm)[b]
50	1	70 ± 0.4
	2	77 ± 3.3
33	1	35 ± 0.6
	2	39 ± 3.3
25	1	13 ± 0.7
	2	19 ± 1.4
	3	23 ± 2.0
	4	26 ± 2.5

[a] Each subsequent coating was deposited after allowing the previous coating to air-dry for 30 min. [b] Film thicknesses were determined by profilometry for samples that were photolithographically patterned before pyrolysis. The uncertainties represent the average thickness variation for three measurements on three different samples.

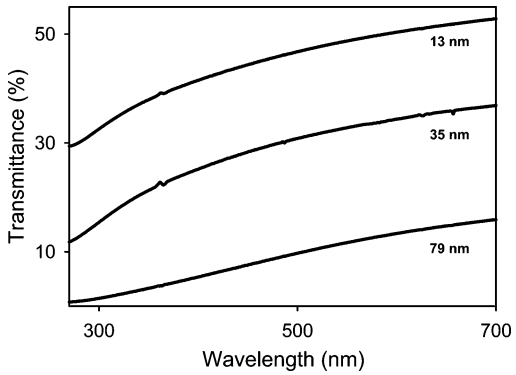

Figure 2. Optical transmittance of C-OTEs as a function of wavelength for three different pyrolyzed film thicknesses.

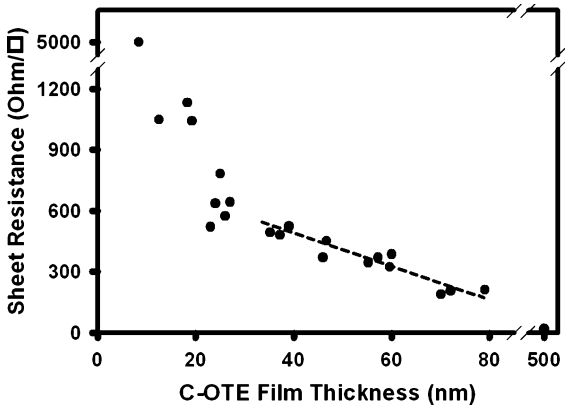

Figure 3. Sheet resistance of C-OTE as a function of pyrolyzed film thickness. The equation for the linear fit to the dependence of the sheet resistance (R_s) and pyrolyzed film thickness (d) between 35 and 80 nm is $R_s = -7.6d + 776$.

detectable increases in thickness (3−7 nm). Comparison of pre- and postpyrolysis film thicknesses indicates that pyrolysis causes a 75−80% decrease in film thickness.

Optical Transparency. Figure 2 displays the optical transmittance from 300 to 700 nm for quartz slides coated with three different thicknesses of pyrolyzed carbon: 13, 35, and 79 nm. The spectra show that (1) transmittance increases as the thickness of the coating decreases and (2) transmittance at a given coating thickness increases as wavelength increases. That is, the 12-nm film has a 33% transmittance at a wavelength of 300 nm, whereas that for the 79-nm film is 1%.

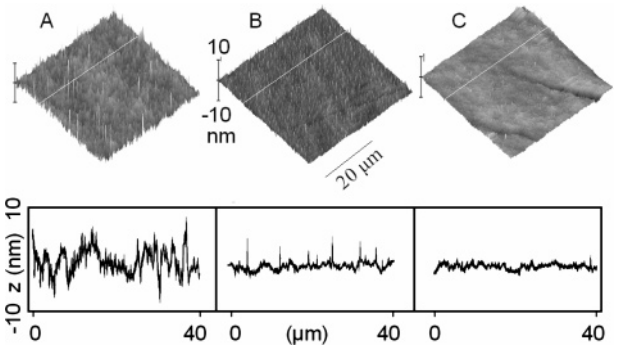

Figure 4. AFM images (40 × 40 μm) and cross-sectional plots of an uncoated quartz substrate (A) and C-OTEs with thicknesses of 18 (B) and 55 nm (C).

In contrast, the transmittance at a wavelength of 700 nm for the 13-nm film reaches 53% and that for the 79-nm film is 27%. These results are consistent with expectations from the wavelength dependencies of carrier absorption and film thickness.[24−27] The transmittance of our C-OTEs is in the same range of other metallic OTEs but is slightly less than that of OTEs such as indium tin oxide.[4,6]

Electrical Conduction. The electrical characteristics of our C-OTEs as a function of film thickness were evaluated via sheet resistance (R_s) measurements with an in-house-constructed four-point probe. These results are presented in Figure 3 for pyrolyzed film thicknesses up to ∼500 nm. As is evident, R_s undergoes a slow increase as the film thickness decreases from ∼500 to ∼35 nm. Below ∼35 nm, however, R_s exhibits a more dramatic increase as thickness decreases. This dependence mimics that for sputter-deposited carbon films,[16] as well as that for ultrathin metal and semiconductor films.[5,28] The basis for the evolution of the electrical properties of our films is briefly examined below.

Last, by incorporating the film thickness into the sheet resistance measurements, the resistivity can be calculated. The average resistivity for C-OTEs that are 35−80 nm thick is 2.4×10^{-3} Ω·cm with a standard deviation of 3.1×10^{-4} Ω·cm, assuming the sheet resistance over these thicknesses follows a linear dependence. This value compares well with the resistivity reported for thick, nontransparent films of pyrolyzed photoresist (5.7×10^{-3} Ω·cm).[20,21]

Material Composition. The elemental composition of the C-OTEs was evaluated via XPS and closely matched that found for the much thicker versions of this material.[20] The Raman spectroscopy analysis revealed that the microcrystalline structure of the C-OTEs is also similar to thick film PPF. A detailed discussion of both sets of data is available as Supporting Information.

Surface Roughness. The surface topography of our C-OTEs was evaluated by tapping mode AFM. Images (40 × 40 μm) are presented in Figure 4 for C-OTEs with thicknesses of 18 and 55 nm, along with an image of an uncoated quartz substrate for comparative purposes. Cross-sectional plots accompany each image. The images show that the underlying substrate is much

(24) Williams, M. W.; Arakawa, E. T. *J. Appl. Phys.* **1972**, *43*, 3460−3463.
(25) Taft, E. A.; Philipp, H. R. *Phys. Rev.* **1965**, *138*, A197−A202.
(26) Greenaway, D. L.; Harbeke, G. *Phys. Rev.* **1969**, *178*, 1340−1348.
(27) Adkins, C. J.; Hamilton, E. M. In *Conduction in Low-Mobility Materials*; Klein, N., Tannhauser, D. S., Pollak, M., Eds.; Taylor & Francis Ltd.: 1971; pp 229−233.
(28) Levchenko, I.; Baranov, O. *Vacuum* **2004**, *72*, 205−210.

rougher than the two carbon-coated samples. The quartz substrate has a large number of spikelike features that extend slightly beyond the scale of the *z*-axis of the image. Based on images from several different quartz substrates, the root-mean-square (rms) roughness of these quartz substrates is ~2.6 nm.

The presence of the spikes diminishes upon the formation of the pyrolyzed film. This decrease is attributed to the conformal behavior of the photoresist during deposition or the melting of the coating in the early stages of heat treatment. As a consequence, the rms roughness of the 18-nm coating is 0.8 nm and that for the 55-nm coating is 0.5 nm. The latter coating therefore exhibits a smoothness that rivals those found at gold films that are prepared by extended annealing and templating procedures.[29−31] These images also show the occasional presence of larger imperfections in the underlying substrate, which we attribute to striations from the final stages of polishing by the manufacturer.

The smoothness of these C-OTEs points to an intriguing explanation for the transition observed in the sheet resistance data in Figure 3. In the growth of thin metal and semiconductor films, the coating forms first as discontinuous islands that eventually coalesce as thickness increases. The resistance of these materials therefore evolves via a percolation model due to the diffuse scattering of carriers at the air/metal and metal/substrate interfaces.[5,28] The AFM images in Figure 4, however, suggest that the pyrolyzed carbon films form a continuous coating even at exceedingly low thicknesses (e.g., 10 nm); there is little evidence for defects or pinholes as would be expected with the island growth process of metallic thin films.[16,27] Interestingly, evaporated carbon films with a continuous structure have been reported for thicknesses as low as 2 nm when formed on the atomically smooth terraces of single crystals.[32] In these cases, the decrease in conductivity associated with decreasing film thickness is attributed to a progressive restriction of hopping conductivity,[27,32−34] a mechanism that may also be operative on our C-OTEs.

Electrochemical Performance. Figure 5 presents steady-state cyclic voltammograms (1 mV/s) for 1.0 mM solutions of hydroxymethylferrocene (HMF) and 1.0 mM ferrocyanide, both in 1.0 M KCl. These curves were collected using a 35-nm C-OTE as the working electrode. The peak separation for HMF/HMF$^+$, a kinetically fast redox couple is close to the reversible value of 60 mV. That for $Fe(CN)_6^{3-/4-}$, which is a slower couple and more sensitive to surface interactions, is much larger at 95 mV.[15,22,35] Scans at higher sweep rates for both systems, however, exhibit much larger peak separations as a consequence in large part of the internal resistance of the exceedingly thin electrode material.[36]

Figure 5 also presents a scan at 1 mV/s in only supporting electrolyte (1.0 M KCl). The response indicates that our C-OTEs have a large accessible potential window, enabling electrochemical

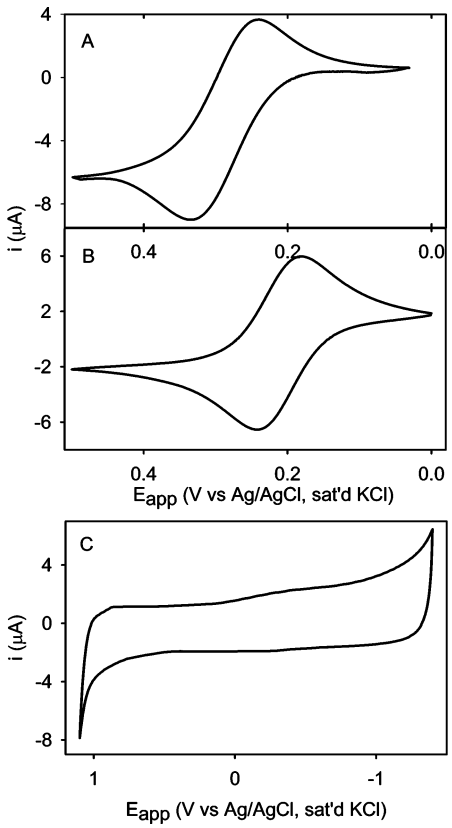

Figure 5. Steady-state cyclic voltammetric responses of a 35-nm C-OTE in (A) 1.0 mM ferrocyanide, (B) 1.0 mM hydroxymethylferrocene, and (C) supporting electrolyte. In all cases, the supporting electrolyte was 1.0 M KCl. RE, Ag/AgCl in saturated KCl; CE, Pt wire; geometric electrode area *A*, 0.28 cm^2. Scan rate, 1 mV/s.

investigation at large anodic and cathodic potentials. The curve also shows a low level of oxygen reduction at −0.4 V.[19] The working potential window of 2 V is similar to that of indium−tin oxide electrodes.[4] It also surpasses that typically accessible with glassy carbon but is a little less than that for doped diamond films.[37] The scan in 1.0 M KCl can also be used to determine the capacitance of the C-OTE/supporting electrolyte interface. This analysis yields a value of 6.5 μF/cm^2, which is on a par with values reported for thick-film electrodes of pyrolyzed photoresist[22] and diamond electrodes.[37]

Spectroelectrochemical Performance. The potential utility of our C-OTEs to follow a change in the spectral characteristics of a redox couple with respect to a change in applied potential was carried out using chronoabsorptometry. This experiment employed an SEC cell of conventional design, 10.0 mM ferrocyanide in 1.0 M KCl as the chromophoric redox probe, a 35-nm-thick C-OTE, and a potential step from 0.00 to +0.60 V. Figure 6 presents the evolution of the spectral response between 370 and 480 nm and shows an increase in absorbance with time, which is consistent with the generation of ferricyanide (λ_{max} = 420 nm; ϵ_{max} = 1020 M^{-1}·cm^{-1}).[38] A linear relationship (correlation coefficient of 0.998) between the change in absorbance (ΔA) and the square root of time ($t^{1/2}$) confirms the effective performance of this material for use in a traditional spectroelectrochemical format

(29) Hegner, M.; Wagner, P.; Semenza, G. *Surf. Sci.* **1993**, *291*, 39−46.
(30) Wagner, P.; Hegner, M.; Guentherodt, H. J.; Semenza, G. *Langmuir* **1995**, *11*, 3867−3875.
(31) Wong, S. S.; Porter, M. D. *J. Electroanal. Chem.* **2000**, *485*, 135−143.
(32) MacVicar, M. L. A. *J. Appl. Phys.* **1970**, *41*, 4765−4768.
(33) McLintock, I. S.; Orr, J. C. In *Chemistry and Physics of Carbon*; Walker, P. L., Thrower, P. A., Eds.; Marcel Dekker: New York, 1973; Vol. 11, pp 243−312.
(34) Morgan, M. *Thin Solid Films* **1971**, *7*, 313−323.
(35) Shporer, M.; Ron, G.; Loewenstein, A.; Navon, G. *Inorg. Chem.* **1965**, *4*, 361−364.
(36) Based on the 35-nm electrode thickness and 0.3-cm working electrode radius, an internal resistance of ~6.1 kΩ was measured.
(37) Witek, M.; Wang, J.; Stotter, J.; Hupert, M.; Haymond; Sonthalia, P.; Swain, G. M. *J. Wide Bandgap Mater.* **2001**, *8*, 171−788.
(38) Porter, M. D.; Kuwana, T. *Anal. Chem.* **1984**, *56*, 529−534.

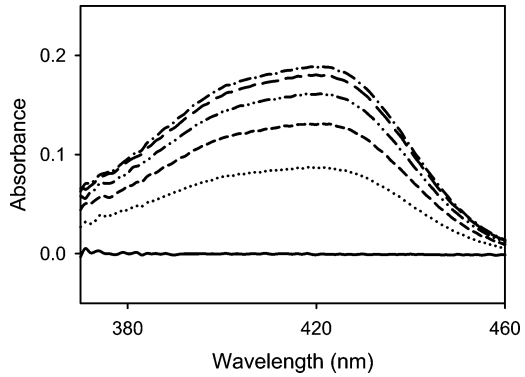

Figure 6. Chronoabsorptometry results for the oxidation of ferrocyanide upon the change in applied potential from 0.00 to +0.60 V.

(i.e., semi-infinite linear diffusion conditions prevail). The equation for the resulting linear plot is $\Delta A = -0.014t^{1/2} + 0.068$.

Single-Molecule Monitoring at Electrified C-OTEs. To probe the potential utility of our C-OTEs as substrates for investigations by single-molecule spectroscopy, the ability to monitor the potential dependence of the adsorption of YOYO-I-labeled λ-DNA was investigated. Since the rate of diffusion for small molecules in water is large, residence times in the evanescent field layer (EFL) are fairly short. Small molecules, as a consequence, appear in the EFL for only one frame at frame rates less than 10 Hz when freely diffusing and not attractively interacting with the surface.[39] It is therefore challenging to track freely diffusing, small molecules from one frame to the next. Much larger biomolecules, like λ-DNA with unpaired bases at the ends that can interact with the surface, however, reside longer within the thin EFL and can be continuously monitored for several consecutive frames, and for an even longer period of time when adsorbed.[23,40] This situation provides a basis for a preliminary assessment of the ability to track the adsorption of individual YOYO-I-labeled λ-DNA at the electrified interface of a C-OTE.

An example of the results from these proof-of-concept tests are presented in the 60 × 80 μm images in Figure 7 (movie 7 in Supporting Information). Figure 7A is an image at the C-OTE/electrolyte interface prior to application of a +1.5-V potential difference between the C-OTE and platinum counter electrode. Each bright spot represents one single tagged λ-DNA molecule in the EFL. In general, most of the molecules are freely diffusing, appearing and disappearing at random locations on successive image frames upon movement in to and out of the EFL. Very few (if any) can be tracked from one frame to the next.

After the application of +1.5 V to the C-OTE, the number of λ-DNA observed in the EFL begins to increase. This increase is evident upon examination of Figures 7B and C, which were obtained 10 and 60 s after voltage application, respectively. The evolution of the images is attributed to the gradual increase in the positive surface charge density of the carbon film, which would result in an increase in the electrostatic attraction with the high, negative charge density of DNA at pH 8.2.[41]

The evolution of these images yields another interesting point. While the apparent number of molecules in the EFL clearly increases, there is little evidence for an increase in residence time for DNA molecules. They are not attached to the surface but freely moving under these low potentials. When the C-OTE is grounded after the +1.5-V experiment, the number of λ-DNA molecules observed is similar to that prior to application of any potential (as in Figure 7A). This result differs from our earlier reports in which λ-DNA, when adsorbed on the surface of thiol-derived monolayers on gold with different terminal groups or on that of a metal oxide, remained fixed on the same location at the surface for a large number (tens to hundreds) of consecutive image frames.[40,41] Studies in which the effect of applied potential and pH, the latter of which can be used to manipulate the charge density on the DNA backbone, are necessary before we can speculate much further as to the basis of this difference.

Further evidence for the potential dependence of adsorption by single-molecule spectroelectrochemistry is presented by the plot in Figure 8. This plot summarizes the number of λ-DNAs

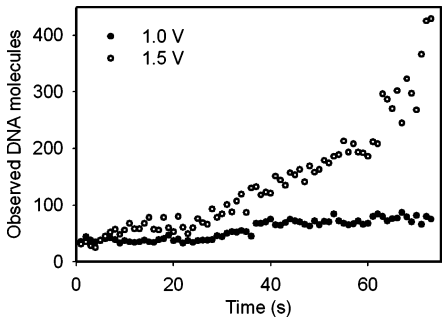

Figure 8. Time dependence of DNA molecules appearing within the evanescent field layer upon applying a potential of 1.0 and 1.5 V.

detectably present in the EFL as a function of time for potential differences of +1.0 and +1.5 V. The plot for +1.5 V shows an increase in the number of observed molecules from an initial level of just under 50 to over 400 within the time course of the

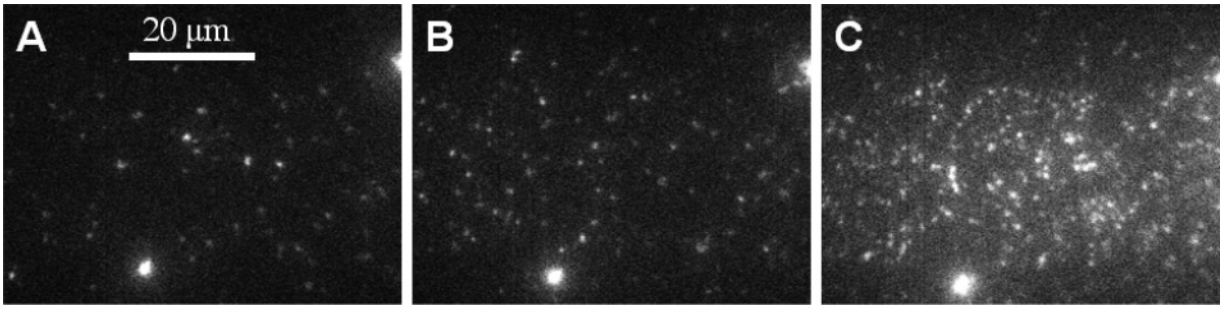

Figure 7. Fluorescent images of YOYO-I-labeled λ-DNA at the C-OTE/aqueous interface: (A) prior to the application of a potential difference between the C-OTE and a platinum counter electrode; (B) 10 and (C) 60 s after application of +1.5 V to the C-OTE. Note that (A) corresponds to 0.45 s into the movie and that (B) and (C) reflect images at 2.89 and 19.97 s into the movie, respectively. The image dimensions are 60 × 80 μm, C-OTE thickness is 35 nm, and the λ-DNA concentration is 50 pM in 10 mM Gly−Gly buffer (pH 8.2).

experiment. Importantly, the plot at +1.0 V is notably different in that the increase is markedly smaller. These contrasting results are qualitatively consistent with the expectation of a larger electrostatic attraction of λ-DNA to the carbon electrode at the more positive value of the potential differences.

In completing this first study, we also examined the effect of a much larger value of potential difference, +5.0 V. The images obtained in this experiment (data not shown) yielded a much greater number of molecules present in the EFL, with a large fraction strongly adsorbed for a number (tens to hundreds) of consecutive image frames. This result is attributed to the oxidation of the C-OTE surface, which then appears to adsorb λ-DNA at a magnitude more like that found at the two types of surfaces used in our earlier reports.[40] Moreover, the oxidation appeared irreversible because grounding the C-OTE had little effect on the strongly adsorbed λ-DNA molecules.

CONCLUSIONS

Dilute solutions of photoresist serve as an excellent starting material for the manufacture of C-OTEs. The thickness of the PPFs can easily be adjusted to fit different applications. Optical transparency is achieved for C-OTEs with a thickness of less than ~80 nm while conductivity is sufficient for films that are thicker than 35 nm. Cleaning is achieved easily without damaging the electrodes. Overall, the C-OTE composition, smoothness, and performance are comparable to thick pyrolyzed photoresist films already utilized by the research community. The mechanical stability, transparency, and conductivity make this form of C-OTEs an interesting alternative to existing OTEs. Efforts to exploit the utility of this system to probe the effect of applied potential by single-molecule spectroelectrochemistry are underway. Studies of adsorption at modified carbon electrodes are also planned.

(39) He, Y.; Li, H. W.; Yeung, E. S. *J. Phys. Chem. B* **2005**, *109*, 8820−8832.
(40) Li, H. W.; Park, H. Y.; Porter, M. D.; Yeung, E. S. *Anal. Chem.* **2005**, *77*, 3256−3260.
(41) Since the actual electrode potential is unknown, the evolution of the images may also arise from a decrease in the negative charge density of the carbon electrode, depending on the location of the potential of zero charge with respect to the applied bias voltage.

ACKNOWLEDGMENT

The authors thank A. Bergren, G. Edwards, D. Gazda, R. Lipert, and R. McCreery for invaluable discussions. This work was supported by the Ames Laboratory—U.S.D.O.E. The Ames Laboratory is operated by Iowa State University under U.S. Department of Energy under contract W-7405-eng-82.

SUPPORTING INFORMATION AVAILABLE

More detailed information on the XPS and Raman analysis. AVI movie as noted in the text and represents a continuous 60-s observation window compressed to 20 s. This material is available free of charge via the Internet at http://pubs.acs.org.

Received for review December 19, 2005. Accepted February 21, 2006.

AC052244D